Dilute solution properties of semiflexible star and ring polymers

Daichi Ida

Department of Polymer Chemistry, Kyoto University, Kyoto, Japan

Correspondence: Dr. D. Ida, Department of Polymer Chemistry, Kyoto University, Katsura, Kyoto 615-8510, Japan.

E-mail: ida@molsci.polym.kyoto-u.ac.jp

ABSTRACT: Our recent theoretical and/or Monte Carlo (MC) studies of dilute solution properties of semiflexible stars and rings are briefly summarized. The theoretical results for the intrinsic viscosity $[\eta]$ of the Kratky–Porod (KP) wormlike three- and four-arm stars are shown, and effects of chain stiffness on $[\eta]$ of the stars are examined. A comparison of the results for $[\eta]$ with those for the effective hydrodynamic radius and the second virial coefficient A_2 in a good solvent was made for the semiflexible three-arm stars. It was found that $[\eta]$ is the most suitable object of study to examine the effects of chain stiffness on average chain dimensions of the stars. As for the rings, the MC results for A_2 of the ideal KP rings, which is related to the intermolecular topological interactions, are presented and then compared with the data in the literature for ring atactic polystyrene (a-PS) at Θ for large molecular weight M (1×10^4—6×10^5). Even for ring a-PS in such a range of M, the effects of chain stiffness were still remarkable. The effects of the intramolecular topological constraints on the mean-square radius of gyration and the scattering function of the KP rings are also discussed.

KEYWORDS: dilute solution properties; ring polymer; star polymer; semiflexible polymer; wormlike chain

RUNNING HEADS: semiflexible star and ring polymers

INTRODUCTION

Dilute solution behavior of polymers is mainly governed by their average chain dimensions in solutions, and therefore is significantly affected by their primary molecular structure (e.g., linear, branched, or ring). Numerous experimental, theoretical, and computational studies have compared the average chain dimensions between linear polymers and star[1–7] or ring ones.[8–30] However, almost all of those studies were made for flexible polymers, where a comparison was made of experimental and/or computational results with conventional Gaussian chain theories; only a few studies were made for semiflexible stars[5–7] and rings,[13–15,28–30] which may be considered to be important in the studies of biopolymers, such as the aggregation behavior of xanthan (a double-helical polysaccharide) in aqueous solutions,[31] the supercoiling behavior of circular DNA,[32] and so on.

Semiflexible polymers, i.e., polymers in the range of the crossover from the rigid-rod limit to the random-coil one cannot be fully described by the Gaussian chain.[15] This is also the case even with typical flexible polymers (e.g., polystyrene), if their molecular weight M is not very large ($\lesssim 10^5$). The discrepancy between the Gaussian chain theories and the experimental results becomes more severe with decreasing M.[15] To build up a comprehensive understanding of the dilute solution behavior of the star and ring polymers in this crossover range, it is necessary to make theoretical and/or computational studies using a polymer chain model appropriate for semiflexible polymers.

Linear polymers in the crossover range may be well described by the Kratky–Porod (KP) wormlike chain model.[15,33] This model is defined as a continuous limit of the freely rotating chain or an elastic wire with bending energy immersed in a thermal bath, whose chain stiffness is measured by the stiffness parameter λ^{-1}, which has the dimension of length.[15] The dimensional properties of the KP chain become a function of the reduced contour length λL ($\propto M$) defined as the contour length L of the KP chain measured in units of λ^{-1}. The limits of $\lambda L \to 0$ and $\lambda L \to \infty$ correspond to the rigid-rod and random-coil limits, respectively. Although the KP chain model may in principle be extended to other kinds of non-linear polymer chains, the only theoretical studies that emerged thus far investigate the mean-square-radius

of gyration $\langle S^2 \rangle$ of the KP stars by Mansfield and Stockmayer[5] and $\langle S^2 \rangle$, the intrinsic viscosity $[\eta]$, and the translational diffusion coefficient D of the KP ring by Yamakawa's group.[13–15]

We recently made theoretical and/or Monte Carlo studies of the dilute solution properties of semiflexible star[34–38] and ring[39,40] polymers using the KP wormlike chain model. In this short review, the results of these studies are briefly summarized.

SEMIFLEXIBLE STARS

This section addresses semiflexible (regular) star polymers. Goodson and Novak synthesized three-arm star poly(n-hexyl isocyanate) (PHIC), which is a typical semiflexible polymer, by living titanium-catalyzed coordination polymerization.[7] The three-arm star PHIC may be regarded as a typical example of semiflexible stars, we then consider mainly semiflexible three-arm stars.

We calculated the intrinsic viscosity $[\eta]$ [35] and the translational diffusion coefficient D [37] of the wormlike three-arm stars. The second virial coefficient A_2 of the three-arm stars in a good solvent was evaluated by MC simulations using the freely rotating chain with the Lennard–Jones 6-12 potential.[36] (Recall that the freely rotating chain becomes identical with the KP chain in the continuous limit.) Furthermore, for comparison, $[\eta]$ of the wormlike four-arm stars was also calculated.[38] We note that $[\eta]$, D, and A_2 in a good solvent are proportional to the effective hydrodynamic volume $V_{\rm H}$ of a polymer chain, the reciprocal of the effective hydrodynamic radius $R_{\rm H}$ of a polymer chain, and the effective volume $V_{\rm E}$ excluded to one chain by the presence of another, respectively. Based these results, we examined effects of chain stiffness on the average chain dimensions of semiflexible star polymers in dilute solutions.

In the following two subsections, we first state the results for $[\eta]$ of the KP three- and four-arm stars and then make a comparison of the behavior of $[\eta]$ with that of other properties $R_{\rm H}$, A_2 in a good solvent, and $\langle S^2 \rangle$ for the three-arm stars.

Intrinsic viscosity

Consider a f-arm star chain ($f = 3$ or 4) composed of $n + 1$ identical spherical beads of diameter $d_{\rm b}$ whose centers are located on the KP (regular) f-arm star of total contour length

L and stiffness parameter λ^{-1}, one bead being put on the branch point and $m = n/f$ beads on each arm. The angle between each pair of the unit vectors tangent to the KP contours at the branch point is fixed to be 120° for $f = 3$ and the tetrahedral angle [$= \cos^{-1}(-1/3) \simeq 109°$] for $f = 4$. The contour distance between the centers of two adjacent beads is set equal to d_b, so that $(n + 1)d_b = L$. This is the touched-bead hydrodynamic model[15,41] for the KP f-arm star.

If we use the Kirkwood–Riseman (KR) approximation,[1,42] the validity of which has been examined preliminarily for the semiflexible stars by MC simulations,[34] and consider effects of the beads of finite volume, the intrinsic viscosity $[\eta]$ of the touched-bead model may be evaluated as a sum of the solution of the KR equation and the contribution of the Einstein spheres.[15,41]

Using of this model and the linear KP touched-bead model, we evaluated $[\eta]$ of the KP f-arm star and also that of the linear KP touched bead model, both having the same L, λ^{-1}, and d_b. Then, the ratio g_η of $[\eta]$ of the star and linear chain is calculated and then the theoretical expression for g_η was obtained in the form,

$$g_\eta(\lambda L,\, \lambda d_b) = g_\eta^0(L/d_b) f(\lambda L)\,, \tag{1}$$

where g_η^0 is the asymptotic value of g_η in the limit of $\lambda L \to 0$ and given by

$$g_\eta^0(L/d_b) = \lim_{\lambda L \to 0} g_\eta(\lambda L, \lambda d_b) \tag{2}$$

The explicit expressions for $g_\eta^0(L/d_b)$ and $f(\lambda L)$ are given by Equations (38) and (39) in ref. 35, respectively, for the KP three-arm star and by Equations (28) and (29) in ref. 38, respectively, for the KP four-arm star. Therefore, we examined the behavior of g_η as a function of λL and λd_b.

Figure 1

Figure 1 shows plots of g_η for the KP three- and four-arm stars, denoted by $g_{\eta,3}$ and $g_{\eta,4}$, respectively, against the logarithm of λL. The dashed and solid curves represent the KP

theoretical values of $g_{\eta,3}$ and $g_{\eta,4}$, respectively, calculated from Equation (1) using the explicit expressions for g_η^0 and $f(\lambda L)$ mentioned above with the indicated values of λd_b. The upper dashed and solid horizontal line segments represent the asymptotic values of 0.90 for the three-arm star and 0.82 for the four-arm star, respectively, in the random-coil limit ($\lambda L \to \infty$).[4] The lower dashed and solid horizontal line segments represent the asymptotic values of 4/9 for the three-arm star and 1/4 for the four-arm star, respectively, in the thin-rod limit ($\lambda L \to 0$ and $L/d_\mathrm{b} \to \infty$). Both $g_{\eta,3}$ and $g_{\eta,4}$ decrease from the corresponding random-coil-limiting value and then increase after passing through a minimum with decreasing λL in the range of λd_b investigated. This minimum is due to the fact that the finite volume of the beads composing the chain (the contribution of the Einstein spheres) is taken into account. The ratios depend remarkably on λd_b, and the minimum value of $g_{\eta,f}$ decreases, approaching the corresponding thin-rod-limiting value, with decreasing λd_b. These results indicate that $[\eta]$ of the star polymers depends largely not only on the chain stiffness but also on the hydrodynamic chain thickness.

Other properties

For the three-arm stars, we made a comparison of the results for $[\eta]$ with those for R_H and A_2 in a good solvent along with the results for $\langle S^2 \rangle$ of the KP stars by Mansfield and Stockmayer.[5]

The quantity R_H was calculated using the relation $R_\mathrm{H} = k_\mathrm{B}T/6\pi\eta_0 D$, where k_B is the Boltzmann constant, T is the absolute temperature, and η_0 is the solvent viscosity; the values of D evaluated using the Kirkwood formula[1,43] with the same model that was used in the case of $[\eta]$. The quantity A_2 was evaluated by MC simulations using the freely rotating chain of bond angle θ with the Lennard–Jones 6-12 potential under a good solvent condition. We then evaluated the ratios g_H and g_{A_2} of R_H and A_2, respectively, of the three-arm stars in a similar manner to that in the case of g_η.

Figure 2

Figure 2 shows plots of g_η, g_H, and g_{A_2} along with the ratio g_S of $\langle S^2 \rangle$ by Mansfield and Stockmayer[5] against the logarithm of λL for the three-arm stars. The value of λd_b used for

the calculations of g_η and $g_{\rm H}$ was set equal to 0.03; this value is nearly equal to that for PHIC. The solid, chain, and dashed curves represent the KP theoretical values of g_η, $g_{\rm H}$, and g_S, respectively. The symbols represents the MC values of g_{A_2} for the freely rotating three-arm stars with $\theta = 109°$ (circles), 165° (triangles), and 175° (squares). The number of bonds of the chains was properly converted to λL.[36] The ratios of g_η and g_S decrease remarkably from the corresponding random-coil-limiting values with decreasing λL, while $g_{\rm H}$ and $g_{\rm A_2}$ are rather insensitive to changes in λL.

These results indicate that an examination of the behavior of g_η and g_S as a function of λL (or M) is required to experimentally clarify the effects of chain stiffness on the dilute solution properties of star polymers. Further, considering the fact that an accurate experimental determination of $\langle S^2 \rangle$ is not easy in the range of small M, where the effects of chain stiffness become remarkable, g_η seems to be the most suitable object of study for such purpose.

SEMIFLEXIBLE RINGS

Next, we consider semiflexible ring polymers. For ring polymers, inter- and intramolecular topological constraints arising only from chain connectivity, which inhibits chains crossing each other, may affect dilute solution properties to some extent. The intermolecular topological constraint, i.e., the so-called topological interaction (TI) works to conserve a given link type between a pair of ring polymers. Then, a repulsive force, in the sense of the potential of mean force, results from the TI between unlinked ring polymers. Consequently, the second virial coefficient A_2 remains positive even for the ideal (unperturbed) rings without excluded volume, as explicitly shown in the MC study made by Frank-Kamenetskii et al.[16,17] Their pioneering work on A_2 of rings was followed by theoretical and MC studies based on the Gaussian chain model, which is valid for very long, flexible ring polymers.[18–22] We note that the exact expression of A_2 for the rigid ring has also been derived.[20] Experimentally, positive values of A_2 were observed for ring atactic polystyrene (a-PS) in cyclohexane at Θ for large M (10^4—10^5)[23–25] and also for ring amylose tris(alkylcarbamate)s, which are semiflexible polymers, in Θ solvents by Terao et al.[29,30] The intramolecular topological constraint works to conserve a type of knot of a single ring polymer introduced during synthesis. The presence

of various types of knots affect equilibrium conformational properties of ring polymers. For example, in the random-coil limit ($\lambda L \to \infty$), $\langle S^2 \rangle$ becomes proportional to $\lambda L^{1.2}$ for rings of the trivial knot (unknotted rings)[20,26,27] and to λL for the rings without the intramolecular topological constraints, the latter relation being as is well known.

Although the KP theories of $\langle S^2 \rangle$, $[\eta]$, and D are available for ring polymers,[13–15] as mentioned in the introduction, all of the theories is developed only for rings without the intramolecular topological constraints. No theoretical study of the distinctive property A_2 of unperturbed semiflexible rings had not been made. We made an MC study[39] of the effects of chain stiffness on A_2 of ideal rings using a discrete version of the KP ring.[44] We also examined effects of the intramolecular topological constraints on the conformational properties, $\langle S^2 \rangle$ [39] and the scattering function $P(k)$[40] as a function of the magnitude k of the scattering vector, for semiflexible rings by comparing the MC results for the KP rings of the trivial knot with those for the KP rings without the intramolecular topological constraints. We note that analytical treatments of the inter- and intramolecular topological constraints are quite difficult; the MC method is proper for the present purpose.

We first show the MC results for A_2 of the ideal KP rings and then make a comparison between the MC results and the experimental data for ring a-PS at Θ.[23–25] Next, the MC results for $\langle S^2 \rangle$ are shown. Finally, we give the MC results for $P(k)$ along with the analytical results for the continuous KP ring without the intramolecular topological constraints.

Second virial coefficient

The MC model used in this study is essentially the same as that proposed by Frank-Kamenetskii et al.,[44] i.e., the ring composed of n infinitely thin bonds of bond length l with the harmonic bending energy $\alpha\theta^2/2k_{\rm B}T$ between two successive bonds, where α is the bending force constant and θ is the angle between the two successive bond vectors. This model becomes identical with the continuous KP ring of total contour length $L = nl$ and stiffness parameter λ^{-1} in the continuous limit (λ^{-1} is related to $\alpha/k_{\rm B}T$).[14,15,44] Using this model, A_2 of the ideal KP rings without excluded volume and the intramolecular topological constraints was evaluated from the potential of mean force calculated on the basis of the Gauss linking number.[45]

For practical convenience, an interpolation formula for A_2 as a function of M with the KP parameters λ^{-1} and M_L, where $M_L = M/L$ is the shift factor as defined as the molecular weight per unit contour length of the KP chain,[15] was constructed based on the MC values so obtained along with the asymptotic relation ($A_2 \propto \lambda L^{-1/2}$ or $M^{-1/2}$) in the random-coil limit and the exact relation $A_2 = N_A L^3/6\pi^2 M^2$, where N_A is the Avogadro constant, in the rigid-ring limit by des Cloizeaux.[20] The interpolation formula is given by

$$A_2 = \frac{4N_A\lambda^{-1}}{{M_L}^2} f(\lambda L) \tag{3}$$

with

$$f(L) = \frac{L}{24\pi^2}[e^{-0.6014L} + 0.5700L(1 + 0.9630L^{1/2} - 0.7345L + 0.4887L^{3/2} + 0.07915L^2)^{-1}]^{3/2} . \tag{4}$$

Figure 3

Figure 3 shows double-logarithmic plots of A_2 (in cm^3mol/g^2) against the weight-average molecular weight M_w for ring a-PS in cyclohexane at the Θ temperature (34.5 or 35 °C). The circles, triangles, and squares represent the experimental data by Roovers and Toporowski,[23] by Takano et al.,[25] and by Huang et al.,[24] respectively. The solid curve represents the KP theoretical values (MC results) calculated from Equations (3) and (4) with $\lambda^{-1} = 16.8$ Å and $M_L = 35.8$ $Å^{-1}$; the values of λ^{-1} and M_L were determined for the linear a-PS under the same solvent condition.[46] The dotted line segment of slope unity represents the theoretical values for the rigid ring[20] calculated also with $M_L = 35.8$ $Å^{-1}$. The KP theoretical values first increase along with the dotted line segment, then deviate downward progressively from this line with increasing M_w (or λL), and finally decreases after passing through a maximum. The present results with the values of the KP model parameters determined previously allow for a qualitative explanation of the behavior of the available literature data for ring a-PS in cyclohexane at Θ, although the theoretical values are slightly larger ($\sim 10^{-5}$ cm^3mol/g^2) than the experimental values. The most important indication is that even for ring a-PS in the range of $1 \times 10^4 \lesssim M_w \lesssim 6 \times 10^5$, A_2 at Θ never obeys the random-coil-limiting law ($A_2 \propto M^{-1/2}$ indicated by the thin solid line). The effects of chain stiffness are still quite remarkable.

We note that Terao et al.[30] have shown that the behavior of A_2 of ring amylose tris(*n*-butylcarbamate) in 2-propanol at 35 °C (Θ) as a function of M_w may be fairly well explained by the present MC results for the ideal KP rings with proper values of λ^{-1} and M_L.

Mean-square radius of gyration

Next, we consider the difference between $\langle S^2 \rangle$ of the KP rings of the trivial knot and that of the rings without the intramolecular topological constraints (i.e., the mixture of the rings of all kinds of knots with the Boltzmann weight of the total potential energy of the rings). The former quantity is denoted by $\langle S^2 \rangle_{\text{t.k.}}$ and the latter quantity is denoted by $\langle S^2 \rangle_{\text{mix}}$. Using the same model as that used in the case of A_2, we calculated $\langle S^2 \rangle_{\text{t.k.}}$ and $\langle S^2 \rangle_{\text{mix}}$ by MC simulations. We distinguished the rings of the trivial knot from other types of rings using the Alexander polynomial.[47]

Figure 4

Figure 4 shows double-logarithmic plots of $\langle S^2 \rangle_{\text{t.k.}} / \langle S^2 \rangle_{\text{mix}}$ against λL. The open circles represent the MC values of the KP rings, and the dots represent the MC values of the freely jointed ring (corresponding to $\alpha / k_B T \to 0$) obtained by Moore et al.[27] All of the data points form a single-composite curve, and $\langle S^2 \rangle_{\text{t.k.}} / \langle S^2 \rangle_{\text{mix}}$ increases monotonically with increasing λL. The $\langle S^2 \rangle_{\text{t.k.}} / \langle S^2 \rangle_{\text{mix}}$ values are almost equal to unity for $\lambda L \lesssim 10$. This is natural consequence from the fact that the fraction of the number of rings of the trivial knot in an ensemble of rings without the intramolecular topological constraints is equal to unity for $\lambda L \lesssim 10$,[39] in other words, the rings of non-trivial knots are rarely generated for stiff rings. Although $\langle S^2 \rangle_{\text{t.k.}} / \langle S^2 \rangle_{\text{mix}}$ is considered to become proportional to $\lambda L^{0.2}$ in the random-coil limit,[20,26,27] it is difficult to derive a definite conclusion from only the present data for $\lambda L \leq 10^3$.

Scattering function

Finally, we give the results for $P(k)$. We evaluate $P(k)$ as a function of k for the KP rings without the intramolecular topological constraints and those of the trivial knot by MC simulations using with the same model as that used in the cases of A_2 and $\langle S^2 \rangle$.

Figure 5

Figure 5 shows plots of $\langle S^2\rangle^{1/2}F(k)$ against $\langle S^2\rangle^{1/2}k$ (the reduced Kratky plot) for the KP rings. The function $F(k)$ is the so-called Kratky function defined by $F(k) = Lk^2P(k)$.[15] The solid and dotted curves represent the MC values of the rings without the intramolecular topological interactions and those of the trivial knot, respectively, with $n = 200$ $(= L/l)$ and with the indicated values of λ^{-1}/l. The corresponding values of $\alpha/k_{\rm B}T$ are 0, 0.3, 1, 3, 10, and 30 (from top to bottom), and the corresponding values of λL are estimated to be 200, 142.0, 77.67, 31.15, 9.823, and 3.315 (from top to bottom). The upper chain curve represents the theoretical values of the Gaussian ring[12] (without the intramolecular topological interactions) of $n = 200$, which corresponds to the MC chain of $\lambda^{-1}/l = 1$ $(\alpha/k_{\rm B}T = 0)$. The lower chain curve represents the theoretical values of the rigid ring[48,49] of $L = 200l$.

The MC values for the rings without the intramolecular topological constraints with $\lambda^{-1}/l = 1$ $(\alpha/k_{\rm B}T = 0)$ agree well with the theoretical values for the Gaussian ring in the range of $\langle S^2\rangle^{1/2}k \lesssim 3$ including the peak location $(\simeq 2)$. The difference for $\langle S^2\rangle^{1/2}k \gtrsim 3$ is due to that in local chain conformation between the freely jointed $(\alpha/k_{\rm B}T = 0)$ and Gaussian rings. With increasing λ^{-1}/l (decreasing λL), the peak in the plot of the MC data slightly shifts to the low $\langle S^2\rangle^{1/2}k$ side and becomes lower. The plot of the MC data for $\lambda^{-1}/l = 60.34$ exhibits a second peak, although not sharp, at $\langle S^2\rangle^{1/2}k \simeq 4.5$ as seen in the plot for the rigid ring.

For $\lambda^{-1}/l \leq 6.421$, the MC values for the rings of the trivial knot are somewhat smaller than those for the corresponding rings without the intramolecular topological constraints in the range of $\langle S^2\rangle^{1/2}k \lesssim 6$ as in the case of the Gaussian rings.[50] The difference in the height of the peak between the two cases becomes smaller with increasing λ^{-1}/l and becomes negligibly small for $\lambda^{-1} = 20.36$ and 60.34 ($\lambda L = 9.823$ and 3.315). The reason for this is the same as that in the case of $\langle S^2\rangle_{\rm t.k.}/\langle S^2\rangle_{\rm mix}$ for $\lambda L \lesssim 10$, as shown in Fig. 4.

For practical convenience, we derive the theoretical expression of $P(k)$ for the continuous KP ring without the intramolecular topological constraints in the first Daniels approxima-

tion.[15,51] The expression is given by

$$P(k) = 2L^{-2} \int_0^L (L-t) \exp\left[-\frac{t(L-t)k^2}{6L}\right] \times \left[1 + \frac{k^2}{12} - \frac{11t(L-t)k^2}{36L^2} - \frac{11t^4(L-t)k^4}{1080L^4} - \frac{11t(L-t)^4k^4}{1080L^4} + \cdots\right] dt \,. \quad (5)$$

[Note that $k^2 = \mathcal{O}(L^{-1})$.] In Fig. 5, the dashed curves represent the corresponding theoretical values calculated from Equation (5) with $\lambda^2\langle S^2\rangle = (\lambda L/12)(1 - \lambda L/7)$ in the first Daniels approximation. The theoretical values agree well with the corresponding MC values in the range of $\langle S^2\rangle^{1/2}k \lesssim 3$, where the peak characteristic of the ring appears, for $\lambda L \gtrsim 10$. We note that in the ranges of $\langle S^2\rangle^{1/2}k \lesssim 3$ and $\lambda L \gtrsim 10$, effects of chain thickness on $P(k)$ are negligibly small.[40]

CONCLUDING REMARKS

We have briefly summarized our recent theoretical and/or MC studies of the dilute solution properties of the semiflexible star and ring polymers based the KP wormlike chain model. The effects of chain stiffness on $[\eta]$, $R_{\rm H}$, and A_2 in a good solvent of the three-arm star and also $[\eta]$ of the four-arm star have been examined. For the rings, the behavior of A_2 arising only from the TI in the range of the crossover from the rigid-ring limit to the random-coil one was clarified. Furthermore, the effects of the intramolecular topological constraints on $\langle S^2\rangle$ and $P(k)$ of the KP rings were also discussed. It must be emphasized that the effects of chain stiffness affect largely the dilute solution behavior not only of linear polymers but also of star and ring polymers and are still remarkable even for typical flexible polymers with large M ($\sim 10^5$).

Finally, some remarks are made on the current situation of the studies of the dilute solution properties of star and ring polymers. Few experimental data of semiflexible stars are available at the present time. Synthesis of semiflexible stars having various chain stiffness over a wide range of M and experimental examinations of their dilute solution behavior are desired. For semiflexible rings, a further progress in the theoretical or computational studies of $[\eta]$ and D is required since the existent KP theories of $[\eta]$ and D are valid only for large λL[13,15] and are developed for the rings without the intramolecular topological constraints.

ACKNOWLEDGMENT

The author wishes to thank all of his coworkers, especially Professor Takenao Yoshizaki and Associate Professor Yo Nakamura, for their active collaborations and for helpful discussions.

(REFERENCES)

1 Yamakawa, H. *Modern Theory of Polymer Solutions* (Harper & Row, New York, 1971). Its electronic edition is available on-line at the URL: `http://www.molsci.polym.kyoto-u.ac.jp/archives/redbook.pdf`

2 Douglas, J. F., Roovers, J., & Freed, K. F. Characterization of branching architecture through "universal" ratios of polymer solution properties. *Macromolecules* **23**, 4168 (1990), and papers cited therein.

3 Nakamura, Y. Dilute solution properties of star and comb polymers. *Kobunshi Ronbunshu* **57**, 530–541 (2000), and papers cited therein.

4 Iruruzun, I. M. Hydrodynamic properties of regular star branched polymer in dilute solution. *J. Polym. Sci., Part B: Polym. Phys.* **35**, 563–567 (1997).

5 Mansfield, M. L. & Stockmayer W. H. Unperturbed dimensions of wormlike stars. *Macromolecules* **13**, 1713–1715 (1980).

6 Zimm, B. H. Monte Carlo calculation of the friction coefficient and viscosity number of wormlike star molecules. *Macromolecules* **17**, 795–798 (1984).

7 Goodson, S. H. & Novak, B. M. Synthesis and characterization of wormlike three-arm poly(*n*-hexyl isocyanate) star polymers. *Macromolecules* **34**, 3849–3855 (2001).

8 Semlyen, J. A. ed. *Cyclic Polymers* (Elsevier, London, 1986).

9 Nakamura, Y. Molecular characteristics of cyclic polymers *Kobunshi* **54**, 809–812 (2005), and papers cited therein.

10 Deguchi, T. The mean square radius of gyration for ring polymers in dilute solution. *Kobunshi Ronbunshu* **68**, 767–772 (2011), and papers cited therein.

11 Hirayama, N., Tsurusaki, K. & Deguchi, T. Comparison between the theoretical and experimental values of the second virial coefficient of ring polymers. *Kobunshi Ronbunshu* **68**, 804–810 (2011), and papers cited therein.

12 Casassa, E. F. Some statistical properties of flexible ring polymers. *J. Polym. Sci. Part A* **3**, 605–614 (1965).

13 Fujii, M. & Yamakawa, H. Moments and transport coefficients of wormlike rings. *Macromolecules* **8**, 792–799 (1975).

14 Shimada, J. & Yamakawa, H. Moments for DNA topoisomers: The helical wormlike chain. *Biopolymers* **27**, 657–673 (1988).

15 Yamakawa, H. *Helical Wormlike Chains in Polymer Solutions* (Springer, Berlin, 1997).

16 Vologodskii, A. V., Lukashin, A. V. & Frank-Kamenetskii, M. D. Topological interaction between polymer chains. *Zh. Eksp. Teor. Fiz.* **67**, 1875–1885 (1974) [*Soviet Phys. JETP* **40**, 932–936 (1975)].

17 Frank-Kamenetskii, M. D., Lukashin, A. V. & Vologodskii, A. V. Statistical mechanics and topology of polymer chains. *Nature* **258**, 398–402 (1975).

18 Iwata, K. & Kimura, T. Topological distribution functions and the second virial coefficients of ring polymers. *J. Chem. Phys.* **74**, 2039–2048 (1981).

19 Iwata, K. Evidence of topological interaction among polymers: A_2 of ring polymers in the Θ-state. *Macromolecules* **18**, 115–116 (1985).

20 des Cloizeaux, J. Ring polymers in solution: topological effects. *J. Phys. Lett.* **42**, L-433–L-436 (1981).

21 Tanaka, F. Osmotic pressure of ring-polymer solutions. *J. Chem. Phys.* **87**, 4201–4206 (1987).

22 Deguchi, T. & Tsurusaki, K. Random knots and links and applications to polymer physics. *Proceedings of Lectures at Knots* **96**, 95–122 (1997).

23 Roovers, J. & Toporowski, P. M. Synthesis of high molecular weight ring polystyrenes. *Macromolecules* **16**, 843–849 (1983).

24 Huang, J., Shen, J., Li, C., & Liu, D. A new theoretical approach to problems of the solution behavior of ring-shaped polymers. *Makromol. Chem.* **192**, 1249–1254 (1991).

25 Takano, A., Kushida, Y., Ohta, Y., Matsuoka, K. & Matsushita, Y. The second virial coefficients of highly-purified ring polystyrenes. *Polymer* **50**, 1300–1303 (2009).

26 Grosberg, A. Y. Critical exponents for random knots. *Phys. Rev. Lett.* **85**, 3858–3861 (2000).

27 Moore, N. T., Lua, R. C. & Grosberg, A. Y. Topologically driven swelling of a polymer loop. *Proc. Natl. Acad. Sci. USA* **101**, 13431–13435 (2004).

28 Terao, K., Asano, N., Kitamura, S. & Sato, T. Rigid cyclic polymer in solution: cycloamylose tris(phenylcarbamate) in 1,4-dioxane and 2-ethoxyethanol. *ACS Macro Lett.* **1**, 1291–1294 (2012).

29 Asano, N., Kitamura, S. & Terao, K. Local conformation and intermolecular interaction of rigid ring polymers are not always the same as the linear analogue: cyclic amylose tris(phenylcarbamate) in Θ solvents. *J. Phys. Chem. B* **117**, 9576–9583 (2013).

30 Terao, K., Shigeuchi, K., Oyamada, K., Kitamura, S. & Sato, T. Solution properties of a cyclic chain having tunable chain stiffness: cyclic amylose tris(*n*-butylcarbamate) in Θ and good solvents. *Macromolecules* **46**, 5355–5362 (2013).

31 Matsuda, Y., Biyajima, Y. & Sato, T. Thermal denaturation, renaturation, and aggregation of a double-helical polysaccharide xanthan in aqueous solution. *Polym. J.* **41**, 526–532 (2009).

32 Vologodskii, A. *Topology and Physics of Circular DNA*. (CRC Press, Boca Raton, 1992).

33 Kratky, O. & Porod, G. Röntgenuntersuchung gelöster fadenmoleküle. *Recl. Trav. Chim. Pay-Bas.* **68**, 1106–1122 (1949).

34 Ida, D. & Yoshizaki, T. A Monte Carlo study of the intrinsic viscosity of semiflexible regular three-arm star polymers. *Polym. J.* **39**, 1373–1382 (2007).

35 Ida, D., Nakamura, Y. & Yoshizaki, T. Intrinsic viscosity of wormlike regular three-arm stars. *Polym. J.* **40**, 256–267 (2008).

36 Ida, D., & Yoshizaki, T. A Monte Carlo study of the second virial coefficient of semiflexible regular three-arm star polymers. *Polym. J.* **40**, 1074–1080 (2008).

37 Ida, D. & Yoshizaki, T. Dilute solution properties of semiflexible regular three-arm star polymers. *Polym. Prep. Jpn.* **58**, 708 (2009).

38 Kaneshima, T., Ida, D., & Yoshizaki, T., Intrinsic viscosity of wormlike regular four-arm stars. *Polym. J.* **44**, 115–120 (2012).

39 Ida, D., Nakatomi, D. & Yoshizaki, T. A Monte Carlo study of the second virial coefficient of semiflexible ring polymers. *Polym. J.* **42**, 735–744 (2010).

40 Tsubouchi, R., Ida, D., Yoshizaki, T., & Yamakawa, H. Scattering function of wormlike rings *Macromolecules* **47**, 1449–1454 (2014).

41 Yoshizaki, T., Nitta, I. & Yamakawa, H. Transport coefficients of helical wormlike chains. 4. Intrinsic viscosity of the touched-bead model. *Macromolecules* **21**, 165–171 (1988).

42 Kirkwood, J. G. & Riseman, J. The intrinsic viscosities and diffusion constants of flexible macromolecules in solution. *J. Chem. Phys.* **16**, 565–573 (1948).

43 Kirkwood, J. G. The general theory of irreversible processes in solutions of macromolecules. *J. Polym. Sci.* **12**, 1–14 (1954).

44 Frank-Kamenetskii, M. D., Lukashin, A. V., Anshelevich, V. V. & Vologodskii, A. V. Torsional and bending rigidity of the double helix from data on small DNA rings. *J. Biomol. Struct. Dynam.* **2**, 1005–1012 (1985).

45 Rolfsen, D., *Knots and Links* (Publish or Perish, Berkeley, 1976).

46 Yamakawa, H. & Yoshizaki, T. A Monte Carlo study of effects of chain stiffness and chain ends on dilute solution behavior of polymers. II. Second virial coefficient. *J. Chem. Phys.* **119**, 1257–1270 (2003).

47 Crowell, R. H. & Fox, R. H., *Introduction to Knot Theory* (Ginn, Boston, 1963).

48 Oster, G. & Riley, D. P. Scattering from cylindrically symmetric systems. *Acta. Cryst.* **5**, 272–276 (1952).

49 Huber, K. & Stockmayer, W. H. First cumulant of the dynamic structure factor for rigid rings. *Polymer* **28**, 1987–1989 (1987).

50 Shimamura, M. K., Kamata, K., Yao, A. & Deguchi, T. Scattering functions of knotted ring polymers. *Phys. Rev. E* **72**, 041804-1–041804-6 (2005).

51 Daniels, H. E. XXI.—The statistical theory of stiff chains. *Proc. Roy. Soc. Ser. A* **63**, 290–311 (1952).

Figure Legends

Figure 1 Plots of $g_{\eta,3}$ and $g_{\eta,4}$ against $\log \lambda L$. The dashed and solid curves represent the KP theoretical values of $g_{\eta,3}$ and $g_{\eta,4}$, respectively, with indicated values of $\lambda d_{\rm b}$. The upper dashed and solid line segments indicate the asymptotic values of 0.90 for the three-arm star and 0.82 for the four-arm star, respectively, in the random-coil limit.[4] The lower dashed and solid horizontal line segments indicate the asymptotic values of 4/9 for the three-arm star and 1/4 for the four-arm star, respectively, in the thin rod limit.

Figure 2 Plots of g_η, $g_{\rm H}$, g_{A_2}, and g_S against $\log \lambda L$ for the three-arm stars. The solid and chain curves represent the KP theoretical values of g_η and $g_{\rm H}$ with $\lambda d_{\rm b} = 0.03$. The symbols represents the MC values of g_{A_2} for the three-arm star freely rotating chains with $\theta = 109^\circ$ (circles), 165° (triangles), and 175° (squares), the number of bonds of the chains being properly converted to λL.[36] The dashed curve represents the KP theoretical values of g_S by Mansfield and Stockmayer.[5]

Figure 3 Double-logarithmic plots of A_2 (in $\rm cm^3 mol/g^2$) against $M_{\rm w}$ for ring a-PS in cyclohexane at Θ. The circles, triangles, and squares represent the experimental data by Roovers and Toporowski,[23] by Takano et al.,[25] and by Huang et al.,[24] respectively. The solid curve represents the KP theoretical values (MC results) calculated with $\lambda^{-1} = 16.8$ Å and $M_{\rm L} = 35.8$ $\rm Å^{-1}$. The dotted line segment of slope unity represents the theoretical values for the rigid ring[20] calculated with $M_{\rm L} = 35.8$ $\rm Å^{-1}$.

Figure 4 Double-logarithmic plots of $\langle S^2 \rangle_{\rm t.k.} / \langle S^2 \rangle_{\rm mix}$ against λL. The open circles represent the MC results for the KP rings. The dots represent the values of the freely jointed ring obtained by Moore et al.[27]

Figure 5 Plots of $\langle S^2 \rangle^{1/2} F(k)$ against $\langle S^2 \rangle^{1/2} k$ for the KP rings. The solid and dotted curves represent the MC results for the KP ring without the intramolecular topological constraints and those for the KP ring of the trivial knot, respectively, with $n = 200$ $(= L/l)$ and with the indicated values of λ^{-1}/l. The upper

and lower chain curves represent the theoretical values for the Gaussian[12] and rigid rings,[48,49] respectively. The dashed curves represent the corresponding theoretical values of the KP rings in the first Daniels approximation.

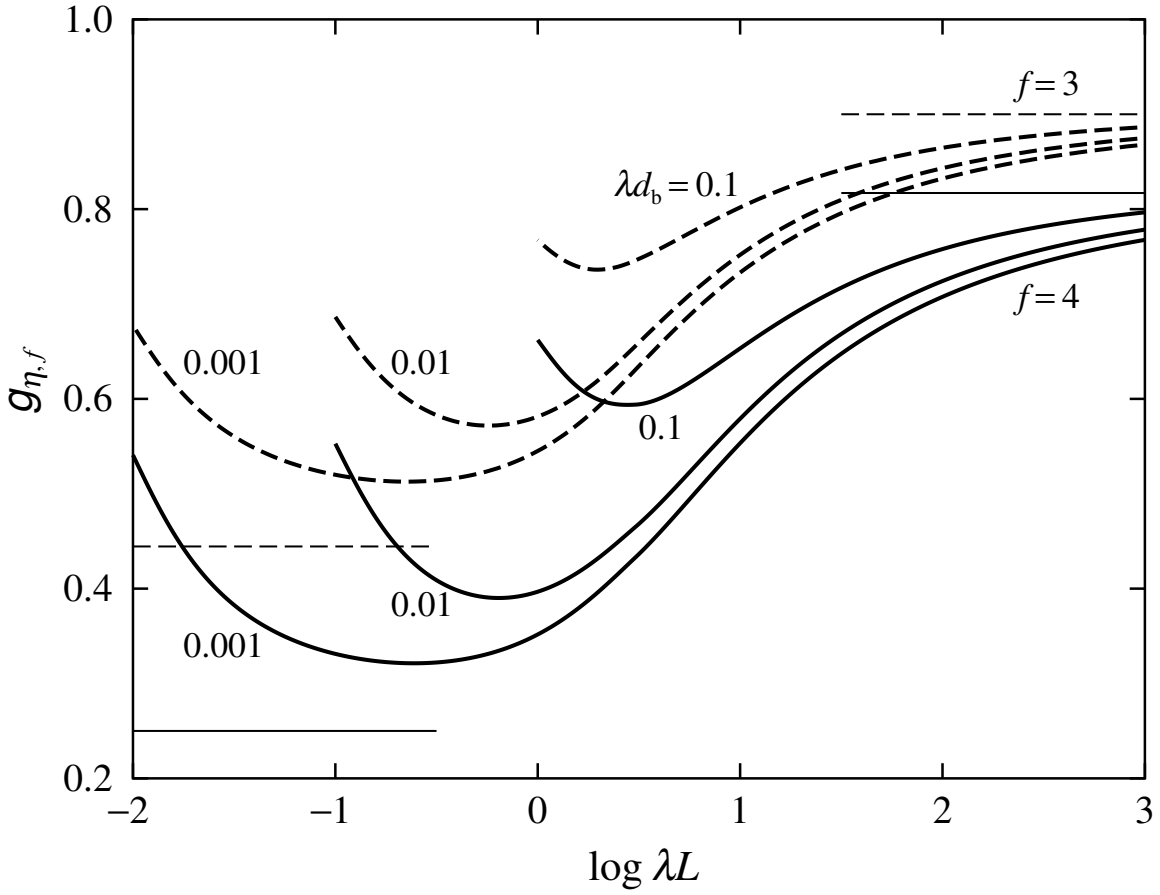

D. Ida, Figure 1

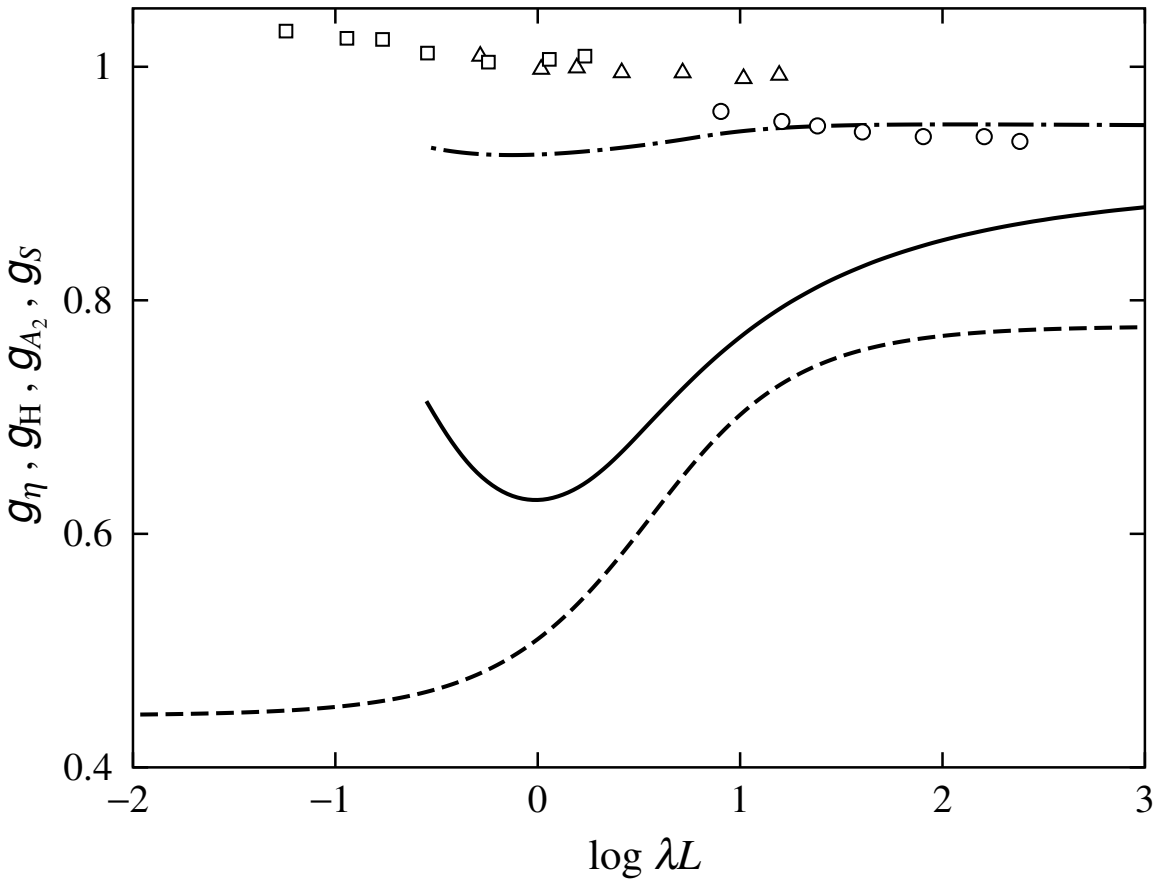

D. Ida, Figure 2

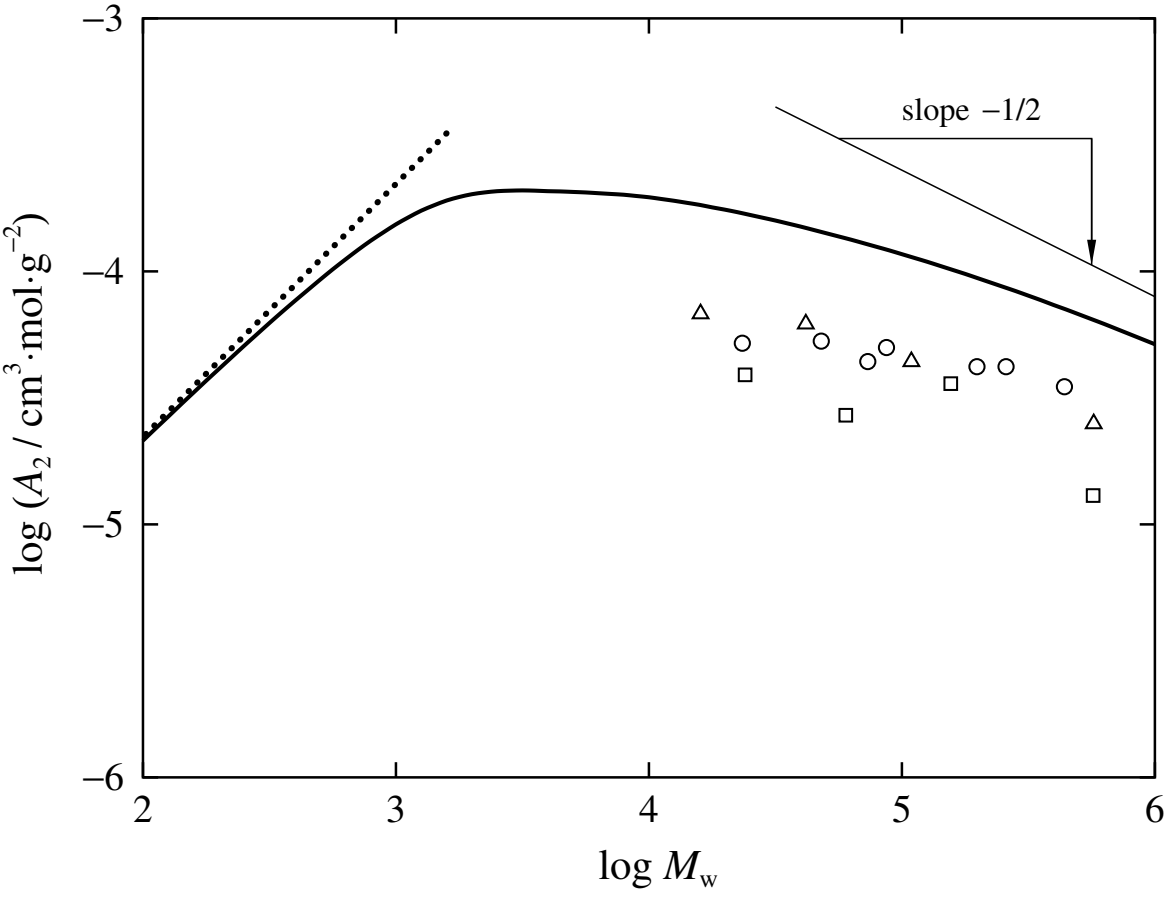

D. Ida, Figure 3

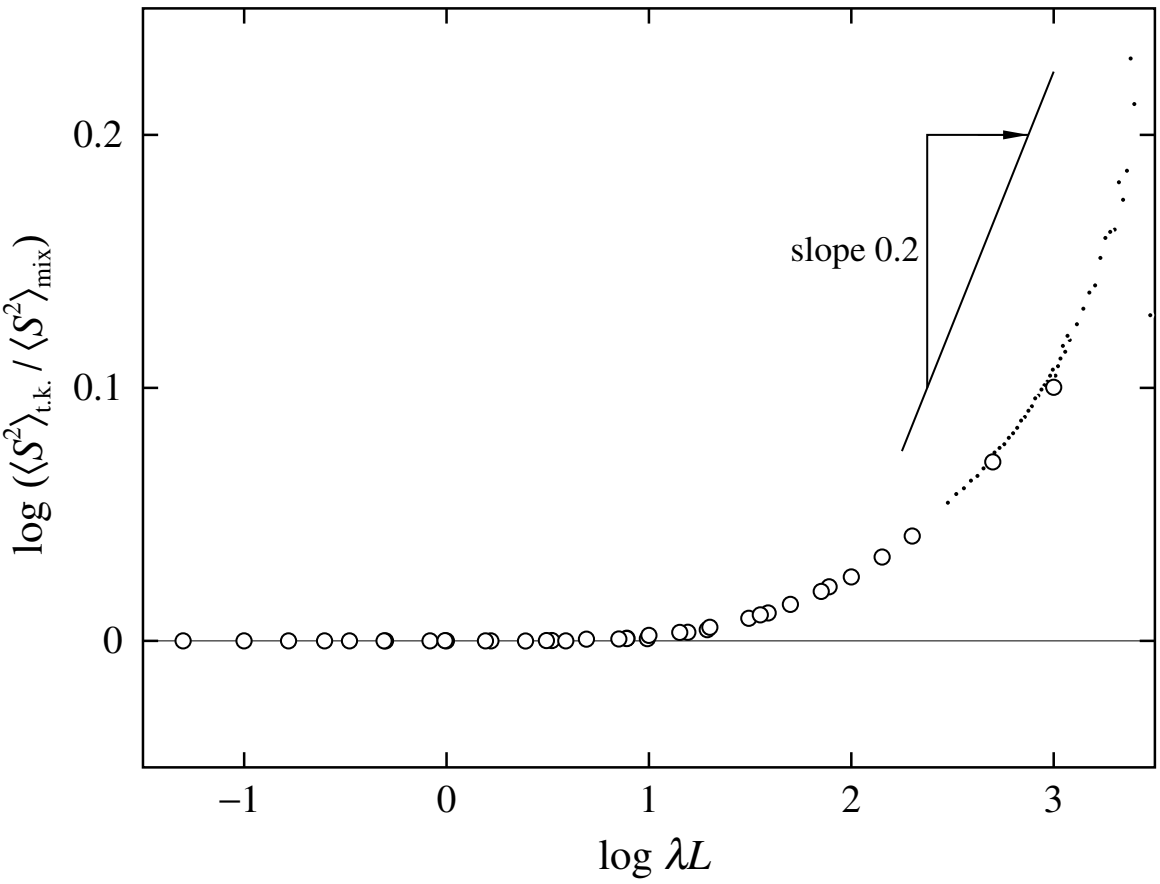

D. Ida, Figure 4

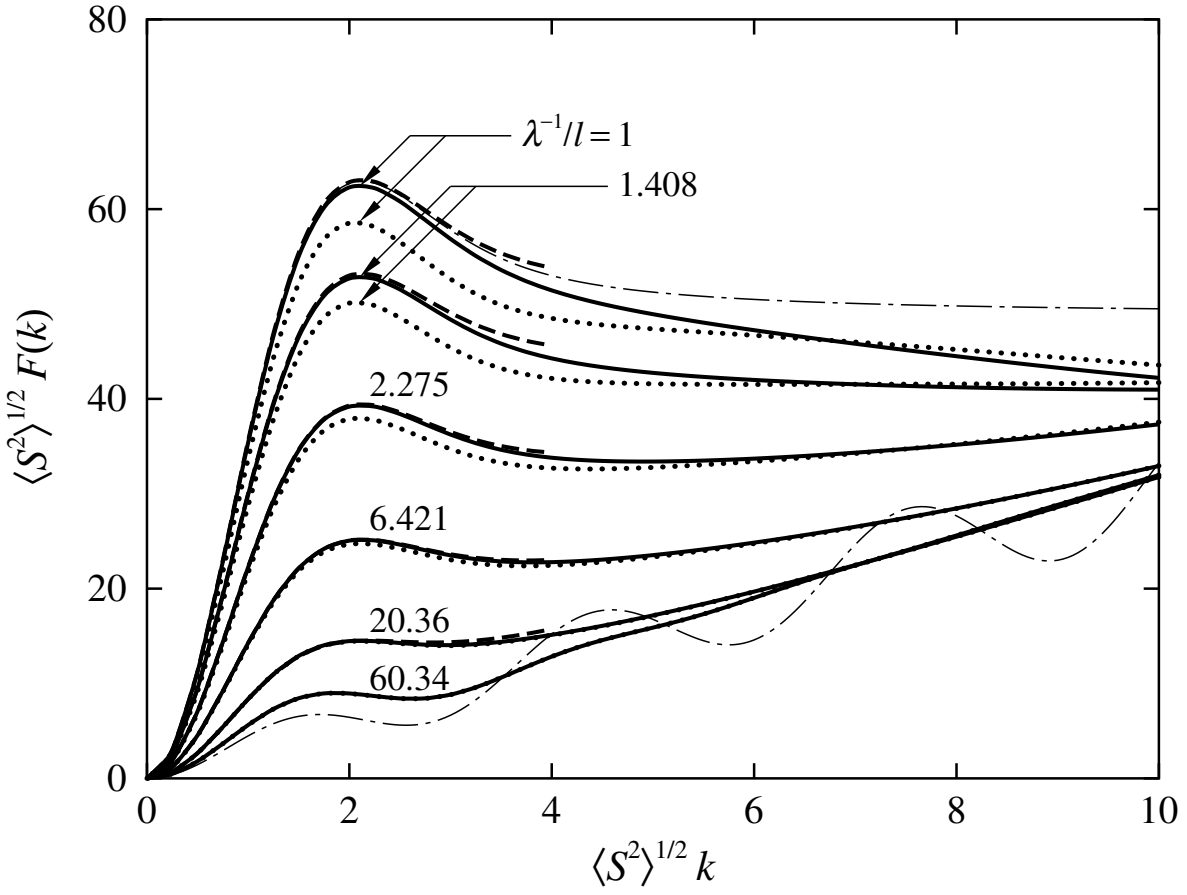

D. Ida, Figure 5